Chapter 3

Experiments and Analysis

3.1 Introduction

Generally speaking, the semiconductor material, insulator surface, and the junction of organic/metal usually dominate the performance of OTFTs. Thus, studying and optimizing these factors are important to have a good device performance.

In the second half of this chapter, we will exam the theory of **Chapter 2.3.3** by introducing CuPc into the OTFTs and the pentacene-based diode.

3.2 Fabrication and Electrical Analysis of Organic TFT Device

The familiar inorganic semiconductor processes, such as growth in one furnace, chemical vapor deposition (CVD), patterning by photo-lithography, and etching, are usually not suitable for the fabrication of OTFTs; therefore, the simple fabrication processes, like thermal deposition and spin casting, are more compatible to OTFTs. Moreover, the simple fabrication processes also make the total cost more effective.

3.2.1 Standard device structure and the transfer characteristics

Most researches on OTFTs use highly-doped silicon substrate (***p***-type or ***n***-type) as the common gate electrode. Thermal growth silicon dioxide (SiO_2) on the highly-doped silicon substrate is used as the insulator. The highly-doped silicon substrate provides high conductivity. Moreover, the thermal growth SiO_2 has compact and uniform structure, which can prevents the defects, reduce the leakage current, and provides smooth surface as well.

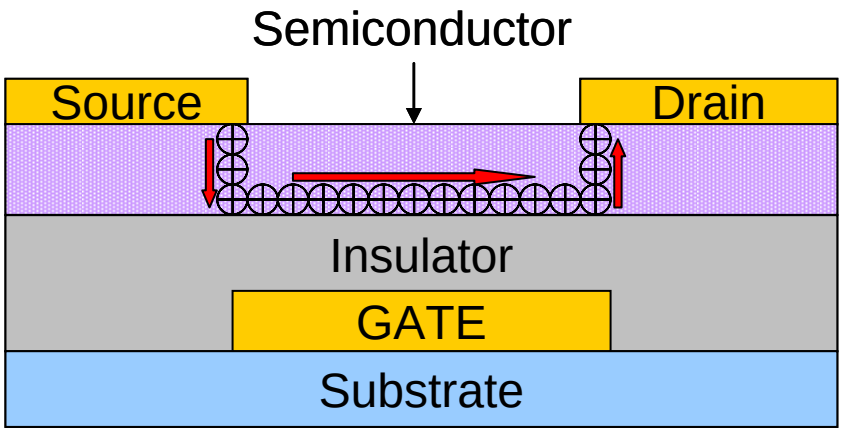

(a)

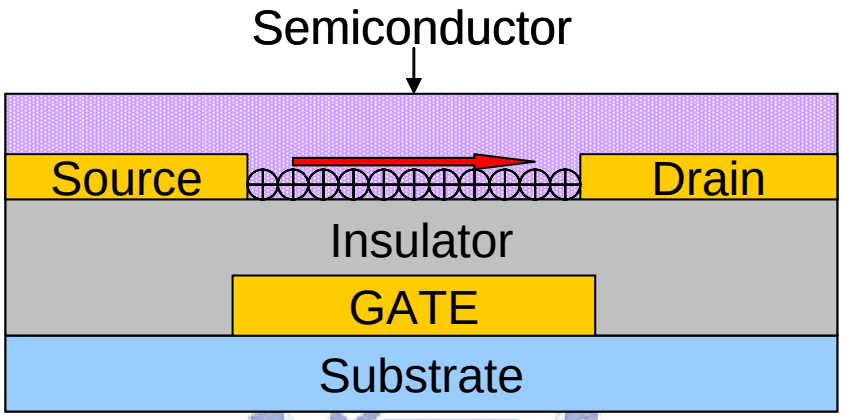

(b)

Fig. 3-1 The operation of (a) Top-Contact and (b) Bottom Contact OTFTs.

In our work, the devices substrates were n-type heavily doped silicon substrate with thermal growth of SiO_2 (2000 Å), which subsequently treated by self-assembly-monolayers (SAMs) as mentioned before.

Pentacene, which was used as received from Aldrich and without any purification, served as the active semiconductor layer. Pentacene (600 Å) was thermally evaporated at a rate of 0.5 Å/s and the deposition substrate temperature was about 25 ^{o}C. The deposition pressure was under 3×10^{-6} Torr.

Gold was evaporated onto the pentacene thin-film as the source and drain electrodes, which was patterned by shadow masking. The channel width was 2 mm and the channel length ranged from 75 μm to 160 μm. The work function of Au, which is close to the HOMO of pentacene, is about 5 eV; thus, Au is a good injection electrode for pentacene-based OTFTs. However, there are energy dipoles between Au electrode and pentacene, which may cause a significant injection barrier (see the detail in **Chapter 2.3**).

For the pentacene-based OTFTs, a negative bias was applied the gate electrons for accumulating holes in ***p***-type active semiconductor. In the $\mathbf{I_D}$-$\mathbf{V_D}$ measurement, shown in Fig. 3-2, the drain bias range from 0 to -60 Volts and the gate bias were 0, -15, -30, -45, and -60 Volts, respectively. In the $\mathbf{I_D}$-$\mathbf{V_G}$ measurement, the gate bias ranges from 20 to -60 Volts and the drain biases were 0, -15 ,-30, -45 , -60 Volts (see Fig. 3-3). Both $\mathbf{I_D}$-$\mathbf{V_D}$ and $\mathbf{I_D}$-$\mathbf{V_G}$ characteristics were measured by Keithley 4200. The linear regime of operation of OTFTs was used to extract the contact resistance by transfer line method (see Chapter 1.3.2). For the linear regime measurement, the drain bias ranged from 0 to -5 Volts for getting linear current-voltage property, and the gate bias were 0, -15, -30, -45, and -60 Volts, respectively (see Fig. 3-4).

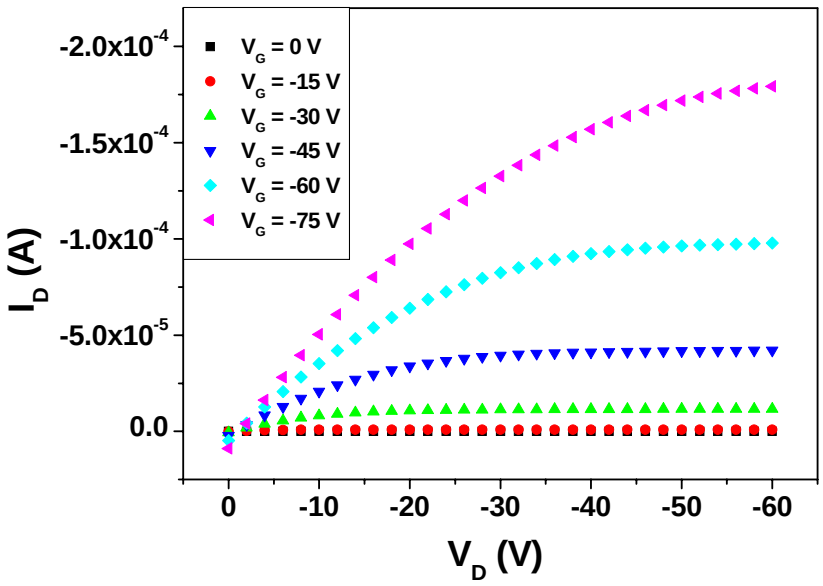

Fig 3-2 The I_D-V_D curve of a standard OTFT.

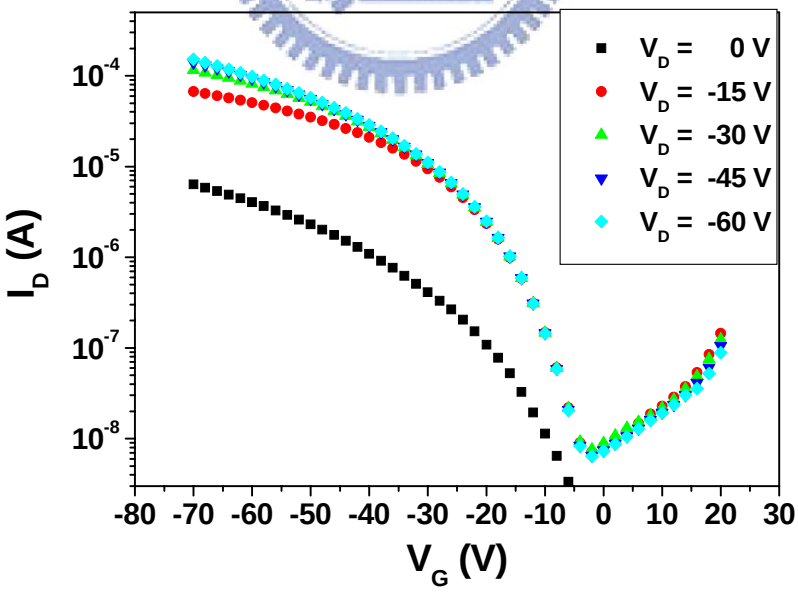

Fig. 3-3 The I_D-V_G curve of a standard OTFT.

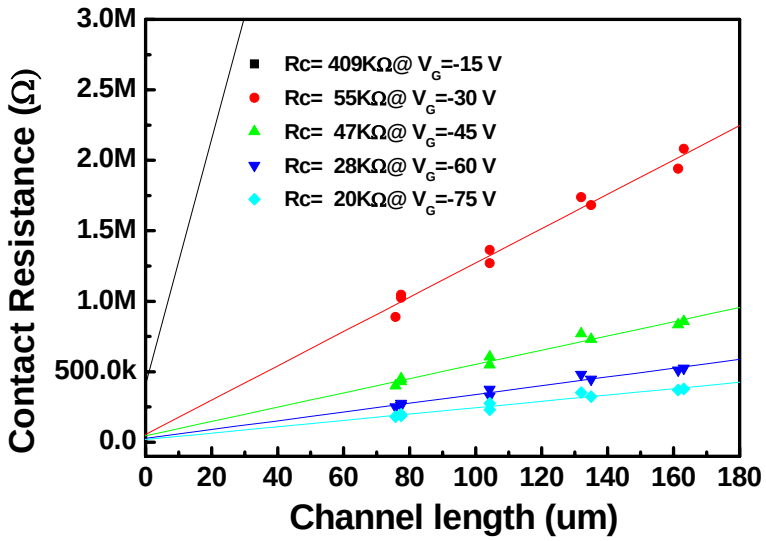

Fig. 3-4 The contact resistance is extracted by transfer line method in the linear regime of the I_D-V_D curve.

3.2.2 The surface treatment of insulator

In the operation of an OTFT, it is widely believed that the current flowing through the gate dielectric/channel interface is dominant (see Fig. 3-1). Therefore, electronic condition at the interface would directly affect the TFT performance.

One of the effective methods to control the condition of the dielectric interface is by surface treatment of the gate insulator [38]. The SiO_2 insulator surface is hydrophilic and is not suitable for the deposition of organic materials, which are usually hydrophobic. Generally speaking, an ordered stack is needed to achieve better charge transport characteristics for organic materials (see the detail in Chapter 2.2). Thus, the idea of modification of SiO_2 terminal modification was applied widely for transforming the hydrophilic SiO_2 surface to a more hydrophobic one.

1,1,1,3,3,3-hexamethyldisilazane (HMDS) is one kind of SAM material, and widely used in the semiconductor industry to improve the adhesion of photoresist on oxide surface.

The HMDS reacts with the oxide surface in a process, which is known as silylation, forming a strong bond to the surface. At the same time free bonds are left which readily react with the photoresist, enhancing the adhesion. As the pentacene was deposited on HMDS-modified SiO_2 surface, a larger grain-size is observed (see Fig. 3-5). Other materials, such as octadecyltrichlorosilane (OTS), and poly-α-methylstyrene (PαMS), are also often used to modify the SiO_2 surfaces. Transfer characteristics of HMDS modified pentacene OTFTs with channel width and length of 2 mm and 75 μm, respectively. And the on/off is more than 10^5 and the mobility is about 0.14 $cm^2V^{-1}s^{-1}$ (see Fig. 3-6).

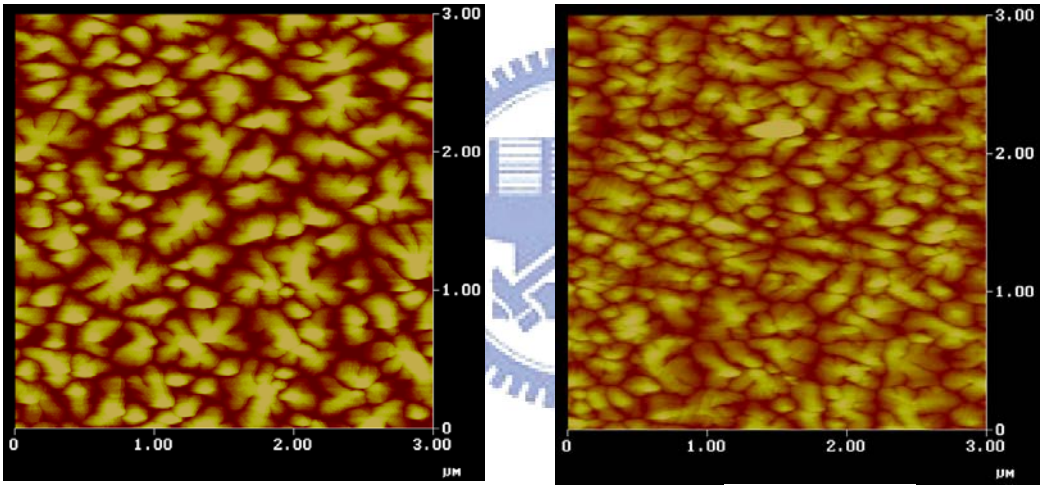

(a) **(b)**

Fig. 3-5 Tapping mode AFM images of (a) larger grain size of pentacene on HMDS modified SiO_2 (b) smaller grain size of pentacene on SiO_2 with no modification.

One PαMS solution, in which toluene is as the solvent, is spin-coated on the surface of SiO_2 at 2000 rpm for 40 seconds. Certainly, the PαMS film is not monolayer. After spin-coating, the PαMS modified substrate was baked at 100 ^oC for 1 hour. Finally, the

prepared substrate was loaded into high-vacuum chamber. Transfer characteristics of PαMS modified pentacene OTFTs with channel width and length of 2 mm and 75 μm, respectively. The on/off is more than 10^6 and the mobility is about 0.5 $cm^2V^{-1}s^{-1}$ (see Fig. 3-7).

For modification with OTS, SiO_2 substrate is dipped into the OTS solution, in which of chloroform and n-hexane is used as the solvent. After dipping for ten seconds, the substrate was picked up and rinsed by n-hexane to obtain a approximate monolayer. Finally, the solution dry naturally and then was loaded into high vacuum chamber. Transfer characteristics of OTS modified pentacene OTFTs with channel width and length of 2 mm and 75 μm, respectively. And the on/off is close to 10^5 and the mobility is 0.42 $cm^2V^{-1}s^{-1}$ (see Fig. 3-8).

Although OTS-modified devices have lower mobility and on-off ratio, compared with PαMS modified devices, the threshold voltage is much lower. Generally speaking, the mobilities of OTS-modified devices are better than others, which suggesting that the optimum modification conditions, such as solution concentration or duration of dipping, may be not yet achieved.

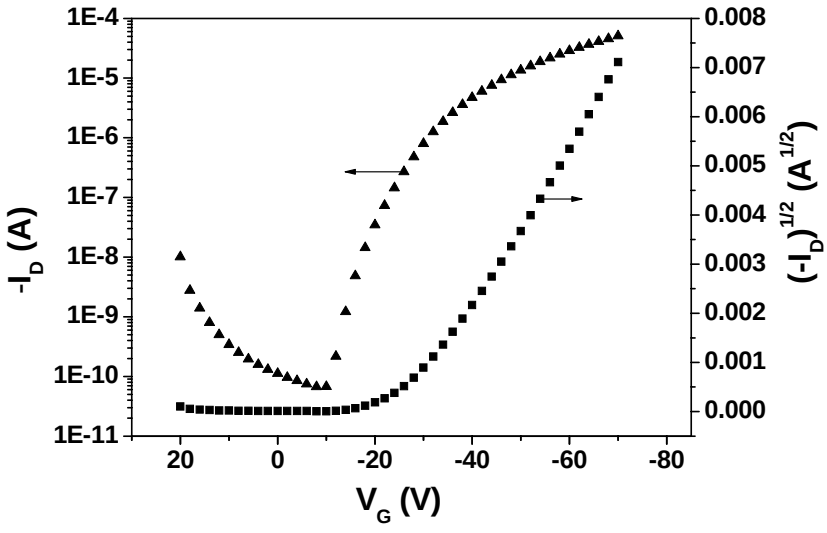

Fig 3-6. Transfer characteristics of HMDS modified pentacene OTFTs.

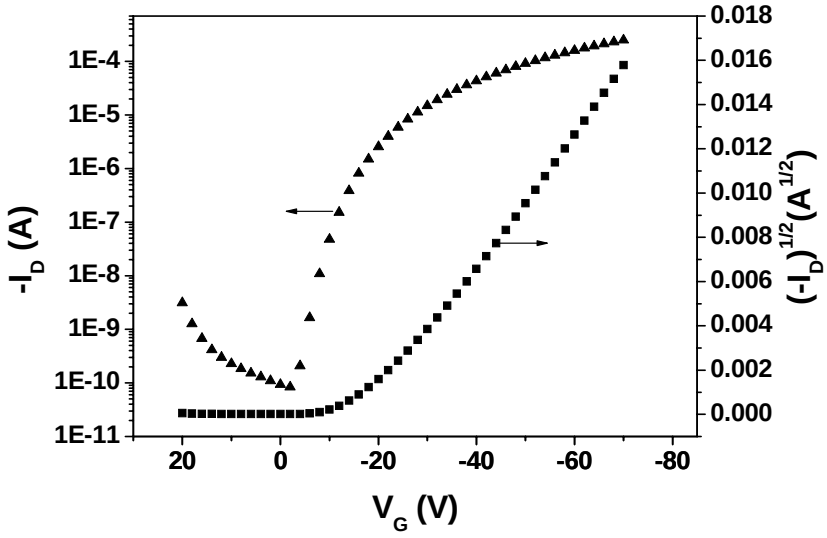

Fig 3-7. Transfer characteristics of P*α*MS modified pentacene OTFTs.

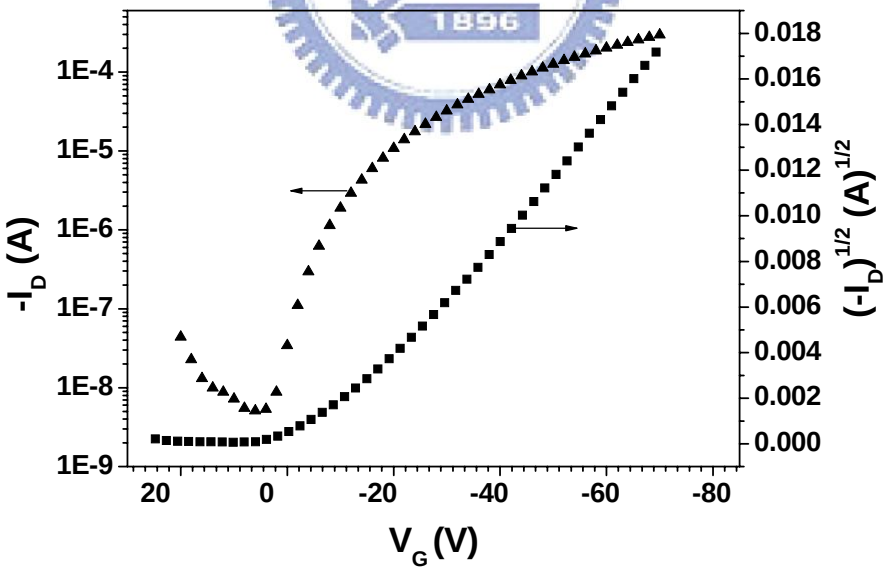

Fig 3-8. Transfer characteristics of OTS modified pentacene OTFTs.

Table 3-1. The comparison of OTFTs with different insulator modification.

	Mobility (cm^2/Vs)	**V_T (V)**	**S.S.** (V/decade)	**On/off**
Pure SiO_2	**< 0.1**	**~ -30**	**~ 5**	**~ 5×10^5**
HMDS	**0.14**	**-26.9**	**~ 3**	**5×10^5**
PαMS	**0.5**	**-19.8**	**~ 2**	**3×10^6**
OTS	**0.42**	**-12**	**~ 3**	**1×10^5**
V_T: threshold voltage, S.S. : sub-threshold slop, On/off : on-off ratio				

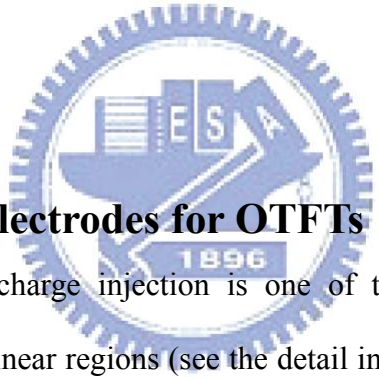

3.3 The Composite Electrodes for OTFTs

It has been reported that charge injection is one of the difficulties to achieve high performance, especially in the linear regions (see the detail in **Chapter 2**). Consequently, it is crucial to develop methods to improve the charge injection efficiency and to lower the contact resistances.

In this work, copper phthalocyanine (CuPc) (Fig. 3-9) was used as the buffer layer to promote the hole injection into the semiconductor layer. It is interesting to see how the 10 Å thin film of CuPc, which is barely with island-like pattern, helps the hole injection apparently. There are some experiments have been done in this section to demonstrate successfully the enhancement of the device performance by the CuPc modification.

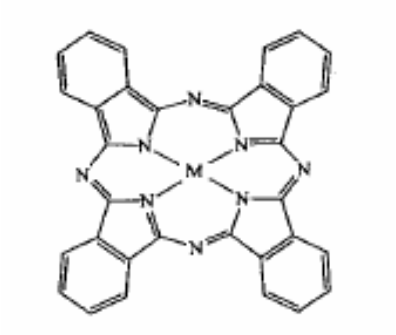

Fig. 3-9 Copper phthalocyanine (CuPc)
(M = Cu)

3.3.1 The comparison between composite electrode and standard device

The composite electrode showed in Fig. 3-10 was made by inserting the CuPc thin film between pentacene active layer and Au electrode. The CuPc thin film was thermally evaporated on pentacene. The deposition rate was 0.5 Å/s and the deposition substrate temperature was about 25°C without any substrate baking. The deposition pressure was under 3×10^{-6} Torr.

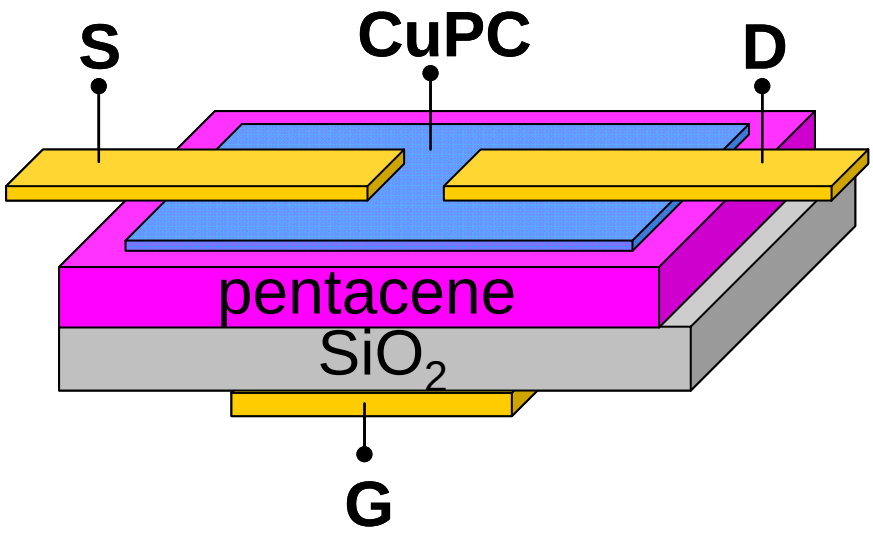

Fig. 3-10 The devices structure of CuPC modified organic TFTs

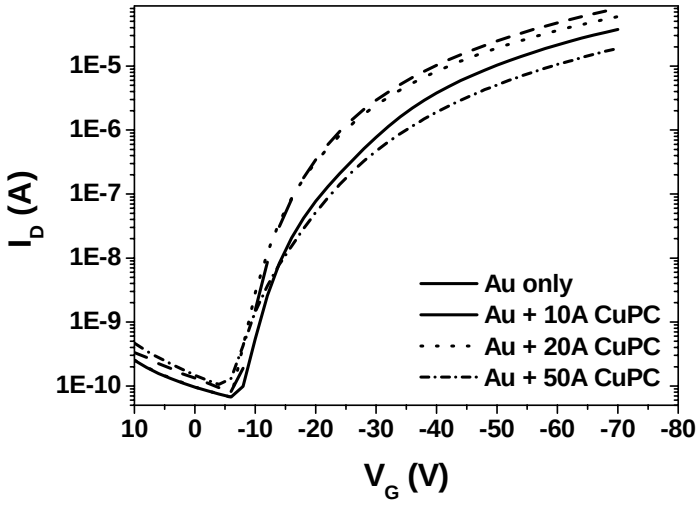

Fig. 3-11 The transfer character of OTFT with electrodes made of Au and Au/CuPC.

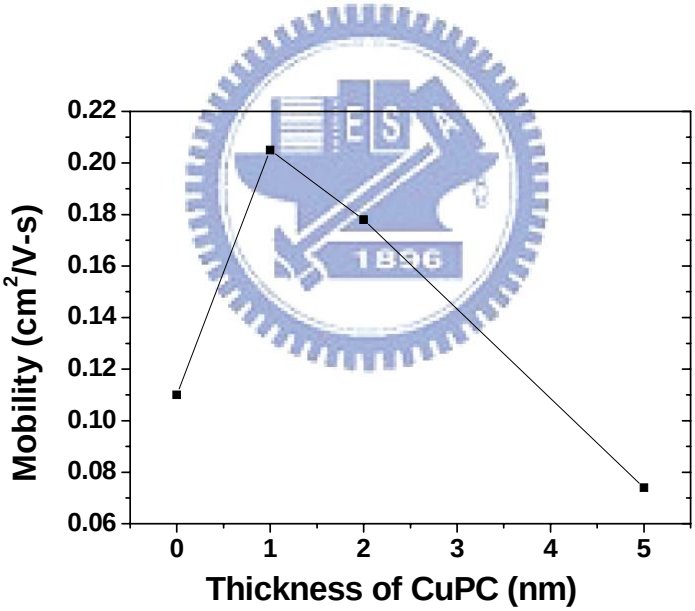

Fig. 3-12 The mobility vs. thickness of CuPc in HMDS modified devices.

In order to clarify the role played by the CuPc, the transfer line method (see Chapter 1) was adapted to estimate the contact resistance from the linear region of current-voltage characteristics. For the device with 10 Å CuPC, the extracted contact resistance was 1.55×10^5 Ω-cm, which is apparently lower than that of the device with pure Au electrodes (4.71×10^5

Ω-cm). The contact resistances of the CuPC-modified devices with different thickness at various gate biases are shown in Fig. 3-13. 10A CuPC caused the contact resistance to decrease by 70 %.

The same transfer characteristic was also observed in the devices modified by PαMS, and OTS. (Fig. 3-14)

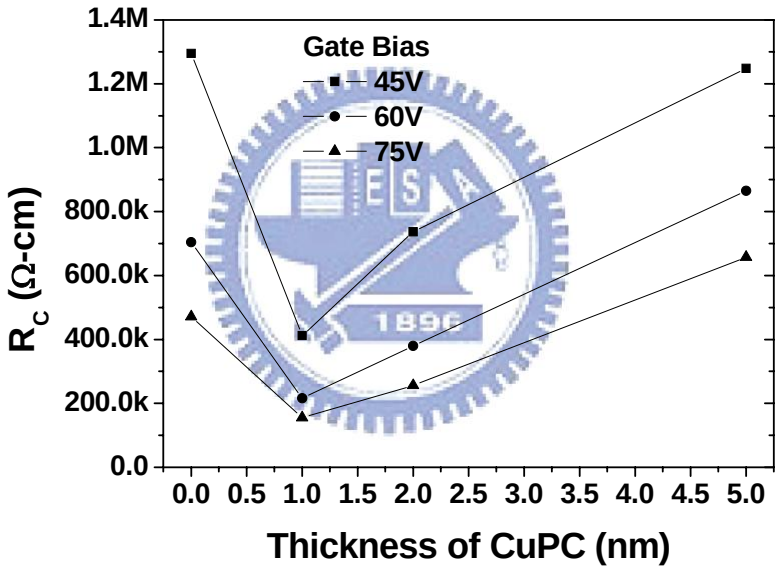

Fig. 3-13 The contact resistance depends on the thickness of CuPC (R_C vs. T).

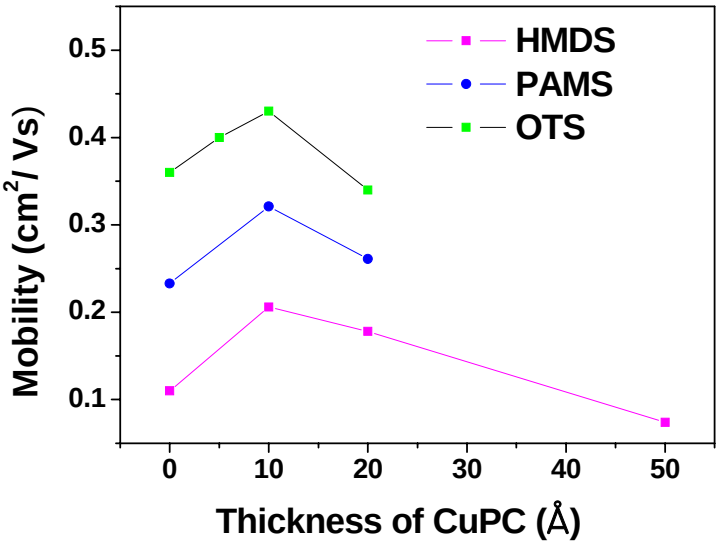

Fig. 3-14 The CuPc modified devices with different insulator treatments. The different surface treatment conditions, such as baking temperature and treating duration, are employed; thus, there are more than one results for each modification material.

Aluminum (Al) has a low work function of 4.0 eV. Thus, Al is usually employed as the electron injection cathode. Fig 3-15 (dash line) shows that the electronic property is bad for Al-only electrode devices. CuPc modified devices are apparently better than that of the device with pure Al electrodes. It implies that the CuPc/Al composite electrodes enhance injection efficiency and decrease the contact resistance. Table 3-2 shows the detail.

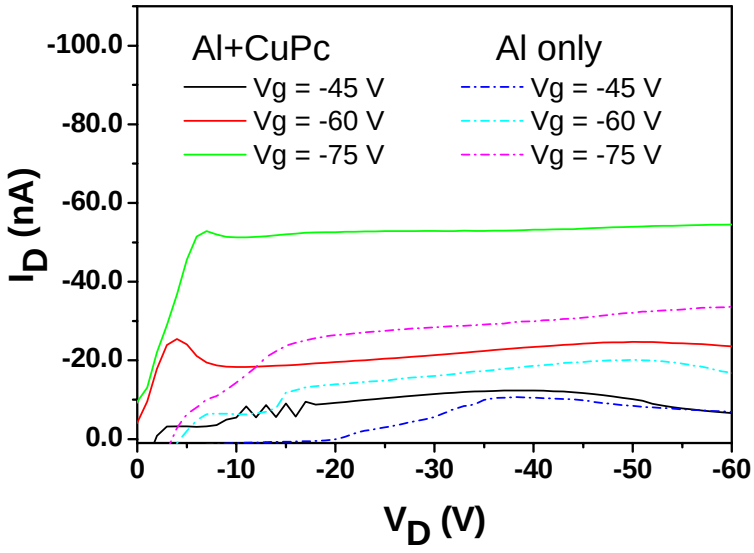

Fig. 3-15 The transfer character of OTFTs with electrodes made of Al and Al/CuPC.

Table 3-2 The comparison of OTFTs with electrodes mode of Al and Al/CuPc.

Electrodes	**Mobility** (cm2/Vs) (Sat. regime)	V_T (V)
Al	**1×10^{-4}**	**- 46**
Al / CuPC	**2×10^{-4}**	**- 37**

3.4 Hole-Only Pentacene-Based Diode

3.4.1 Introduction

The pentacene-based hole-only diode were prepared to verify the hole injection efficiency of the Au anode with and without CuPc modification. It is noted that hole injection from PEDOT/PSS contacts into organic materials is more efficient than from Au contacts, albeit the similar work function of both electrode surface [38]. The electronic structure asymmetry was observed in Au/pentacene/Au structure. This complicated energy diagram would be the obstacle for realizing the injection Au/CuPc composite electrode [39]. (Fig.3-16)

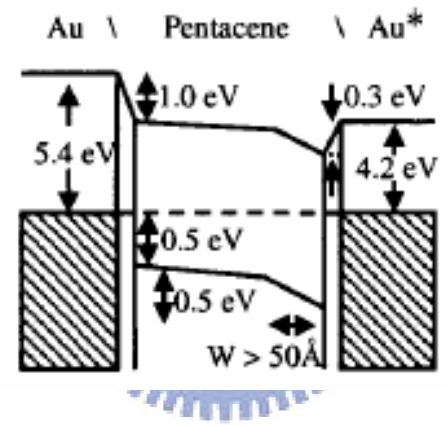

Fig. 3-16 Energy diagrams of the various interfaces between pentacene and Au. The sequence of deposition is from left to right. (Reprint from [39])

3.4.2 Experiments

The structure of pentacene-based diode is shown in Fig. 3-17. First, glass ITO-substrates were cleaned with acetone and detergent for one and three times respectively and then glass was rinsed by de-ion water (DH_2O) and isopropyl alcohol. Finally, the glass was cleaned in

DH_2O twice by ultrasonic vibration. Prior to the PEDOT/PSS deposition, UV-ozone treatment is applied for surface cleaning and work-function alignment of ITO.

PEDOT/PSS was spin-casted from a queous solution onto the cleaned ITO glass and was annealed (120^{o}C) in air for more than an hour. After the annealing, these substrates were loaded into a custom-made vacuum chamber followed by thermally evaporating 2000Å pentacene (deposition rate = 1 Å /s as the pressure lower than $3x10^{-6}$ Torr) as the active layer of this diode. Devices with different thickness of CuPc (0, 1, 2 and 5 nm, respectively) were made. Finally, the gold anode was deposited and patterned by shadow mask. The energy diagram of the hole-only device is shown in Fig. 3-18.

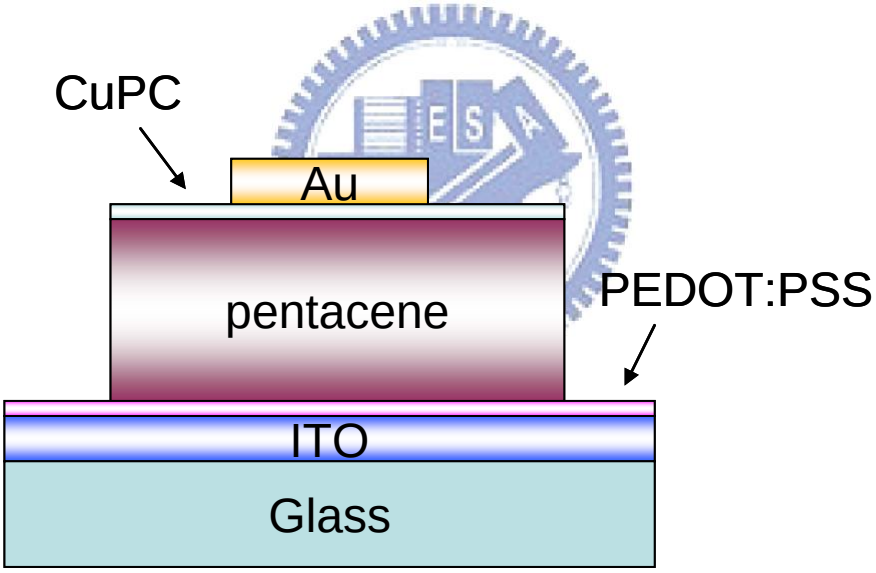

Fig. 3-17 The structure of hole-only pentacene diode which was fabricated on ITO coated glass.

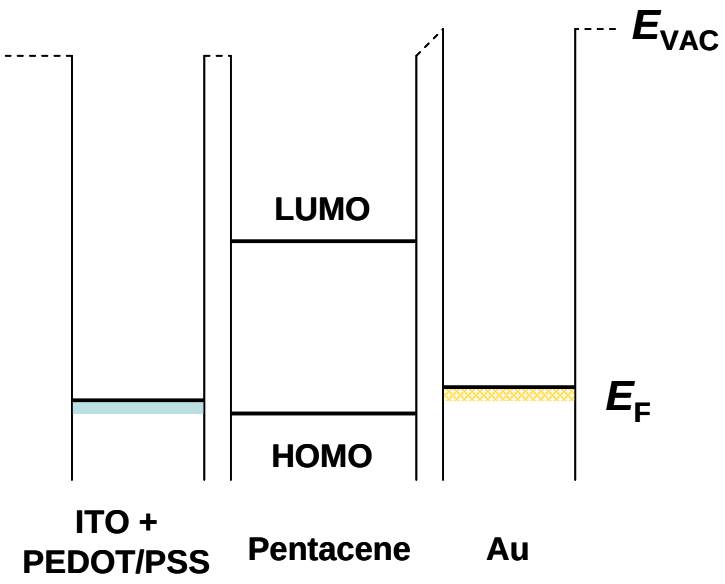

Fig. 3-18 The energy diagram of the hole-only diode.

3.4.3 Results and Discussion

From Fig. 3-19, there is not any significant difference among these current-voltage relations in turn-on regime. The current-voltage relation in the off regime follows the Ohmic law. The turn-on voltage can be extracted by the following method.

The turn-on voltage is located between the sections of off current and on current. First, two lines were drew to approximate to the two set of statistics of the two interval 0 ~ 2 V and 8 ~ 10 V, respectively. Then, extending and intersecting these two lines at one point, which is defined as turn-on voltage (see Fig. 3-20). It is interesting that the turn-on voltage decreases as the CuPc film was inserted between pentacene and gold. Moreover, when a thicker CuPc (> 10 Å) was inserted, the turn-on voltage increases dramatically. (see Fig. 3-21) This phenomenon is agreed with the tendency of contact resistance with different thickness of CuPc. The tendency is also the evidence that the charge injection is improved by CuPc is modification.

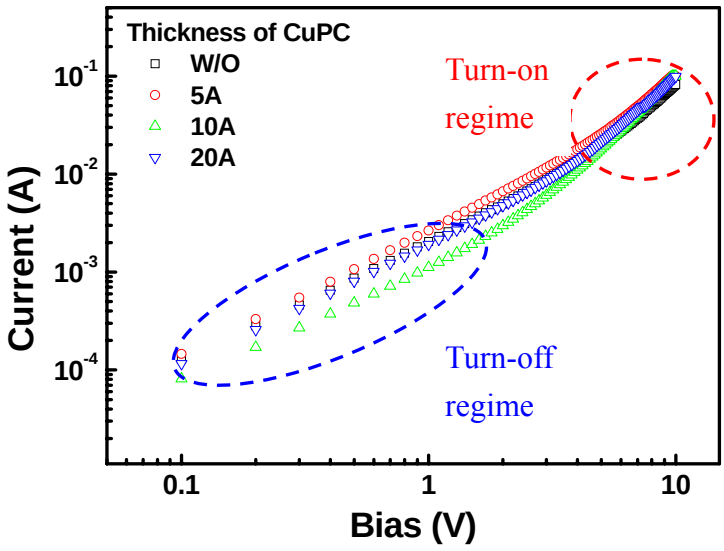

Fig. 3-19 The pentacene-based diode with X-Y logarithm axes.

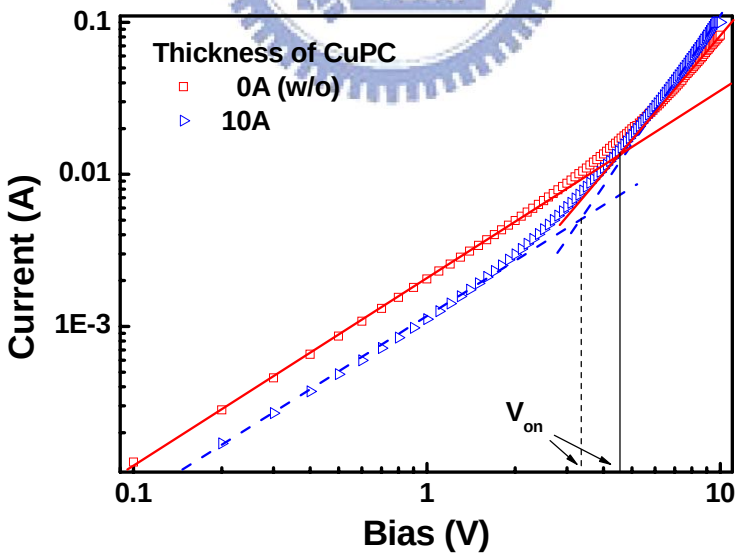

Fig. 3-20 The plot that shows the extraction of turn-on voltage.

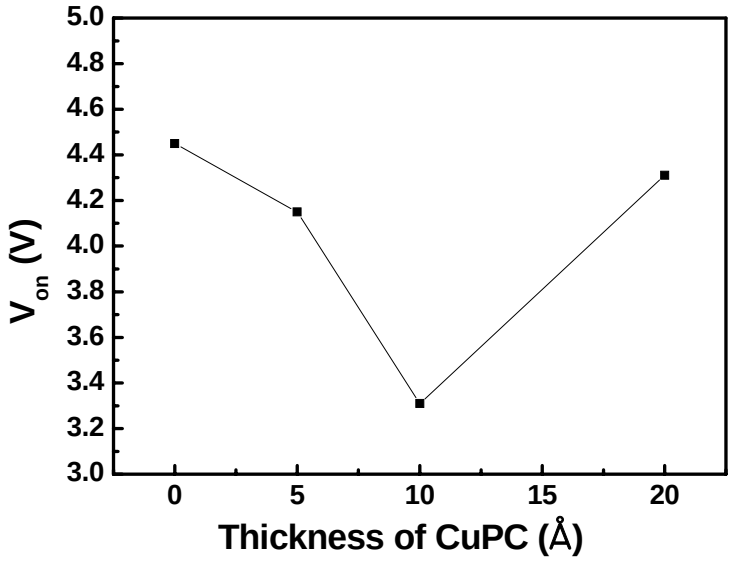

Fig. 3-21 Thickness of CuPc vs. turn-on voltage (V_{on}). This figure shows that the turn-on voltage reduces as CuPc is inserted in pentacene-based diodes.

3.5 Discussion

The surface treatments do transform the hydrophilic SiO_2 terminal to hydrophobic one. Therefore, the surface is more suitable for the pentacene growth. And the electrical properties are also improved vastly, such as the mobility, S.S., threshold voltage, and on/off ratio. (Table 3-1)

It has been demonstrated successfully that the performance of OTFTs can be improved by reducing the contact resistance. For HMDS-modified devices, the contact resistance was decreased by 70% after the modification, deduced from the line-transfer method. The mobility was improved by 86%. This phenomenon is also observed in the other devices modified by PαMS, and OTS (see Fig. 3-14). In addition, the higher current and the lower turn-on voltage in the hole-only diode incorporating with a thin layer of CuPc suggests the improvement of

hole-injection efficiency (see Fig. 3-21). Finally, it is inferred that the lower injection barrier is resulted from the induced gap states at the Au/CuPC interfaces (see Fig 2-7).

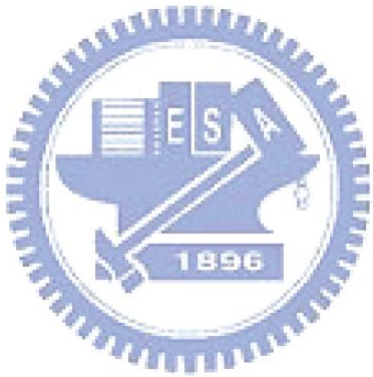

Chapter 4

Conclusion

In the beginning of this thesis, we introduce the progress and the basic understanding of organic TFTs. The well-known and superior semiconductor material “pentacene” and top contact organic TFT are concerned. The thorough studies of the energy construction of organic material are arranged in Chapter 2, and further, we figure out the research aim of novel composite electrode for decreasing the injection barrier by inserting CuPC.

The surface treatments do transform the hydrophilic SiO_2 terminal to hydrophobic one. The PαMS modified organic TFTs show a higher mobility, lower sub-threshold slop, and higher on-off ratio (see Table 3.1).

The Au/CuPc electrodes reduce the contact resistance and improve the mobility of OTFTs. The turn-on voltage of hole-only pentacene-based diode is also reduced by inserting CuPc thin-film. These strong evidences demonstrate the following conclusion. A new gap state is induced due to this charge transfer. As a result, the Fermi level is pinned at the unoccupied gap state [40]. Consequently, the injection barrier is smaller between Au and CuPc (Fig. 2-11b). If we assume no interface dipole is formed between CuPc and pentacene, due to their similar electron-donating natures, the injection barrier indeed lowered by incorporating one thin layer of CuPc. On the other hand, CuPc itself is an intrinsically low-mobility material. Once the thickness of CuPc increases, the bulk resistance of CuPc will contribute to the device, and make the device characters degraded.

Reference

[1] M. Pope, C. E. Swenberg, Electronic Process in Organic Crystals and polymers, 2nd ed., Oxford University Press, Oxford 1999.

[2] H. Shirakawa, E. J. Louis, A. G. MacDiarmid, C. K. Chiang, A. J. Heeger. Synthesis of electrically conducting polymers: halogen derivatives of polyacetylene. *J Chem Soc Chem Commun*. 578 (1997).

[3] F. Ebisawa, T. Kurosawa, S. Nara, *J. Appl. Phys*. **54**, 3255 (1983).

[4] A. Tsumura, K. Koezuka, T. Ando, *Appl. Phys. Lett*. **49**, 1210 (1956)

[5] G. Horowitz, X. Z. Peng, D. Fichou, F. Garnier, *J. Mol. Electron*. **7**, 85 (1991).

[6] C. D. Dimitrakopoulos, A. R. Brown, A. Pomp. *J Appl. Phys*. **80**, 2501 (1996).

[7] J. G. Laquindanum, H. E. Kat, A. J. Lovinger, A. Dodabalapur, *Chem. Mater*. **8**, 2542 (1996).

[8] D. J. Gundlach,Y. Y. Lin, T. N. Nackson, S. F. Nelson, D. G. *Scholm. IEEE Electron Dev. Lett*. **18**, 87 (1997).

[9] S. F. Nelson, Y. Y. Lin, D. J. Gundlach, T. N. Nackson. *Appl. Phys. Lett*. 72,1854 (1998).

[10] M.P. Hong, B. S. Kim, Y. U. Lee, K. K. Song, J. H. Oh, J. H. Kim, S. Y.Lee, B. W. Koo, J. H. Shin, E. J. Jeong, and L. S. Pu, *SID* 2005, 23.

[11] S. F. Nelson et al., *Appl. Phys. Lett*. **72**, 1854 (1998).

[12] H. Klauk, et al., *Solid State Technol*. **43**, 63 (2000).

[13] C. D. Dimitrakopoulos, *Science* **283**, 822 (1999).

[14] C. D. Dimitrakopoulos, D. J. Mascaro, *IBM*, **45**, 11 (2001).

[15] R. B. Campbell, J. monteath Robertson, J. Trotter, *Acta. Cryst.* **14**, 705 (1961).

[16] J. Zaumseil, K. W. Baldwin, and J. A. Rogers, *J. Appl. Phys.* **93** , 6117 (2003)

[17] C. D. Dimitrakopoulos, J. Kymissis, S. Purushothaman, in Proceedings of The Int. Conf.

on Digital Printing Technologies, NIP16, Society of Imaging Science and Technology, Vancouver 2000, 493.

[18] C. D. Dimitrakopoulos, P. R. L. Malenfant, *Adv. Mater*. **14**, 99 (2002).

[19] G. Horowitz, P. Lang, M. Mottaghi, H. Aubin, *Adv. Funct. Mater*. **14**, 1070 (2004)

[20] P. V. Necliudov, M. S. Shur, D. J. Gundlach, Thomas N. Jackson, *Solid-State Electron.* **47**, 259 (2003).

[21] C. W. Tang, S. A. VanSlyke, *App. Phys. Lett*. **51**, 913 (1987).

[22] T. Tani, Photographic Sensitivity, Oxford University Press, *Oxford* (1995).

[23] N. C. Greenham, R. H. Friend, Semiconductor Device Physics of Conjugated Polymers, Academic, New York 1995.

[24] C. W. Tang, *Appl Phys. Lett*. **48**, 183 (1986).\

[25] H. Ishii, K. Sugiyama, E. Ito, K Seki, *Adv. Mater*. **11**, 605 (1999).

[26] M. Pope, C. E. Swenberg, "*Electronic processes in organic crystal and polymers,' 2nd ed*, New York: Oxford University Press 1999.

[27] S. F. Nelson, Y. Y. Lin, D. J. Gundlach, T. N. Jackson, *App. Phys. Lett*. **72**, 1854 (1998).

[28] W. Warta, R. Stehle, N. Karl, *Appl. Phys. A*, **36**, 170 (1985).

[29] N. Karl, J. Marktanner, R. Stehle, W. Warta, *Synthetic Metals*, **41**, 2473 (1991).

[30] N. Karl, "Charge-carrier mobility in organic crystal," In:R. Farchioni, G. Grosso, eds. Organic Electronic Materials, Springer Series in Materials Science, **41**, 283 (2001).

[31] E. A. Hilinsh, V. Capek, Organic Molecular Crystals: Interaction Localization and Transport Phenomena, Chapter 7. New York: American Institute of Physics Press (1994).

[32] N. Karl, Organic Semiconductors, In: O. Madelung, ed. Landolt-Bornstein, Group III, Semicondcutors. **17**, 106 (1985).

[33] S. M. Sze, Physics of Semiconductor Devices, Wiley, New York (1981).

[34] G. Horowitz, F. Dellofre, F Garnier, R. Hajlaoui, M Hmyene, and A. Yassar, *Synth, Met*.

54, 435 (1993).

[35] C. P. Jarrett, R. Friend, A. R. Brown, D. M. de Leeuw, *J. Appl. Phys.* **77**, 6289 (1995).

[36] N. Koch, A. Kahn, J. Ghijsen, J.–J. Pireaux, j. Schwartz, R. L. Johnson, A. Elschner, *Appl. Phys. Lett*. **82**, 70 (2003).

[37] N. J. Watkins, L Yan, S. Zorba, Y Gao, *Proc. of SPIE*, **4800**, 248 (2003).

[38] J. Park, M. Cho, H. B. Park, T. J. Park, S. W. Lee, S. H. Hong, D. S. Jeong, C. LeeC. S. Hwang, *Appl. Phys. Lett*. 13, 5965 (2004)

[39] K. Noch, A. Elschner, J. Schwartz, A. Kahn, *Appl. Phys. Lett*. **82**, 2281 (2003).

[40] L. Lozzi, S. Santucci, S. L. Rosa, *J. Vac. Sci. Technol*. **22**, 1477 (2004).